
OVER 100-FOLD IMPROVEMENT IN THE ACCURACY OF RELAXED EDDY ACCUMULATION FLUX ESTIMATES THROUGH ERROR DIFFUSION

This is a preprint - final version available at <https://doi.org/10.1016/j.agrformet.2024.110207>

✉ **Anas Emad***

Bioclimatology
University of Göttingen
Büsgenweg 2, 37077
Göttingen, Germany
anas.emad@uni-goettingen.de

August 30, 2024

ABSTRACT

Measurements of atmosphere-surface exchange are largely limited by the availability of fast-response gas analyzers; this limitation hampers our understanding of the role of terrestrial ecosystems in atmospheric chemistry and global change. Current micrometeorological methods, compatible with slow-response gas analyzers, are difficult to implement, or rely on empirical parameters that introduce large systematic errors.

Here, we develop a new micrometeorological method, optimized for slow-response gas analyzers, that directly measures exchange rates of different atmospheric constituents, with minimal requirements. The new method requires only the sampling of air at a constant rate and directing it into one of two reservoirs, depending on the direction of the vertical wind velocity. An integral component of the new technique is an error diffusion algorithm that minimizes the biases in the measured fluxes and achieves direct flux estimates.

We demonstrate that the new method provides an unbiased estimate of the flux, with accuracy within 0.1% of the reference eddy covariance flux, and importantly, allows for significant enhancements in the signal-to-noise ratio of measured scalars without compromising accuracy. Our new method provides a simple and reliable way to address complex environmental questions and offers a promising avenue for advancing our understanding of ecological systems and atmospheric chemistry.

Keywords Micrometeorology · land-atmosphere interactions · conditional sampling · atmospheric-exchange · slow-response sensors

1 Introduction

Surface exchange rates or fluxes of different atmospheric constituents are key metrics for investigating and understanding the interactions between the atmosphere and the biosphere [Baldocchi, 2020]. The uncertainty over the distribution of atmospheric species emissions and losses at Earth's surface poses a major limitation to our understanding of atmospheric chemistry and the role of the terrestrial surface in global climate [Arneeth et al., 2010]. Flux studies provide valuable insights into the cycling of trace elements like CO₂, monitor the emission and deposition of pollutants for public health and air quality research,

and contribute to better representation of different atmospheric constituents in climate models [Scholes et al., 2003, Fowler et al., 2009].

Micrometeorological methods are employed to measure atmospheric exchange in the lower atmosphere near the surface, where the transport is predominantly turbulent, causing gases to diffuse rapidly from and to the surface. The flux near the surface is determined as the average of the product of the vertical wind velocity w and the scalar concentration c , \overline{wc} , where the overline denotes the average over a period of time (typically 30 minutes to 1 hour). The direct calculation of the flux \overline{wc}

using the eddy covariance method, is widely recognized as the most direct and reliable way for measuring atmospheric fluxes at the scale of plant canopies [Dabberdt et al., 1993, Hicks and Baldocchi, 2020].

Atmospheric exchange occurs over various spatial and temporal scales, requiring high-frequency measurements (above 10 Hz) of wind velocity and scalar concentration to capture all flux-carrying motions. This high sampling requirement has limited the eddy covariance method to few atmospheric constituents, like water vapor and carbon dioxide, which have fast-response gas analyzers. Yet, many constituents critical to atmospheric chemistry and ecosystem research, such as stable isotopes, nitrogen oxides, and volatile organic compounds, only have slow-response analyzers. For these, several alternative micrometeorological methods compatible with slower analyzers have been developed [Rinne et al., 2021]. Among these alternatives, the true eddy accumulation (TEA) method offers a direct and accurate way to measure the flux $\overline{w\bar{c}}$ without requiring fast-response analyzers. TEA achieves this by sampling air with a mass proportional to the vertical wind velocity and then directing it into one of two reservoirs based on the vertical wind direction. Therefore, the product $w \times c$ is realized physically by proportional sampling and the mean is achieved by sample accumulation. The flux is then calculated from the accumulated mass difference between the two reservoirs [Desjardins, 1977, Hicks and McMillen, 1984]. However, the accurate and fast control of air mass flow rate at the necessary dynamic range required for TEA implementation presents a significant challenge. This has limited the number of successful implementations of the TEA method and has prevented its widespread adoption [Siebicke and Emad, 2019]. A simplification of the eddy accumulation method that does not require proportional mass flow control was proposed by Businger and Oncley [1990], which draws parallels to flux gradient methods by linking the flux with the difference between mean updraft and downdraft scalar concentrations. Unlike TEA, the relaxed eddy accumulation method (REA) does not require proportional mass flow control; instead, air samples are collected at a constant flow rate into updraft and downdraft reservoirs depending on vertical wind direction. The flux in REA is found as the product of the difference between mean accumulated scalar concentrations (ΔC), wind standard deviation (σ_w), and an empirical coefficient β . The interpretation and determination of the empirical coefficient β have remained the primary questions concerning the REA method [Baker, 2000, Yukio and Masahiro, 2004, Fotiadi et al., 2005, Ruppert et al., 2006, Katul et al., 2018, Vogl et al., 2021]. While the theoretical value of β derived assuming a Gaussian distribution for wind and scalar is $\beta \approx 0.63$ [Wyngaard and Moeng, 1992], observed average values of β typically range between 0.47 and 0.63 and exhibit substantial run-to-run variability [Gao, 1995, Katul et al., 1996, Tsai et al., 2012, Grelle and Keck, 2021]. These variations are attributed to diverse stability conditions, scalars, and site-specific factors [Sakabe et al., 2014, Ammann and Meixner, 2002]. The absence of a reliable method for estimating or parametrizing β has made it a major source of uncertainty in REA flux measurements, potentially introducing biases of up to 20% of the flux [Oncley et al., 1993, Gao, 1995].

Despite the high measurement uncertainty associated with the variability of the coefficient β , the REA method remains widely used for atmospheric exchange measurements due to its simple implementation requirements and its ability to increase scalar signal-to-noise ratios by excluding lower wind speeds using a deadband. REA has been applied to measure the fluxes of a wide array of atmospheric constituents. These include stable isotopes, hydrocarbons, methane, volatile organic compounds, ammonia, sulfate, nitrous oxide, mercury, aerosol numbers and dry deposition, halocarbon fluxes, peroxyacetyl nitrate, sodium chloride particle, and benthic solute fluxes in aquatic environments [Beverland et al., 1996, Haapanala et al., 2006, Bowling et al., 1999, Zhu et al., 1999, Pattey et al., 1999, Ciccioli et al., 2003, Matsuda et al., 2015, Hensen et al., 2009, Grelle and Keck, 2021, Skov et al., 2006, Meyers et al., 2006, Osterwalder et al., 2016, Held et al., 2008, Grönholm et al., 2007, Hornsby et al., 2009, Ren et al., 2011, Moravek et al., 2014, Meskhidze et al., 2018, Calabro-Souza et al., 2023, Riederer et al., 2014].

In this paper, we propose a new direct eddy accumulation method that combines the simple requirements of relaxed eddy accumulation with the accuracy and robustness of the conventional eddy covariance technique. The new method employs error diffusion to achieve reliable and direct flux estimates with minimal bias. We begin with a novel theoretical derivation of conditional sampling, formulating sample accumulation as a quantization problem and demonstrating that relaxed eddy accumulation is a special case of this formulation. We identify an unaccounted portion of the flux in the REA method arising from the correlation of the quantization error with the scalar concentration. We then introduce an error diffusion algorithm to randomize this quantization error, leading to unbiased flux estimates. This is followed by a detailed examination of the signal and noise shaping properties of error diffusion and a discussion of how it effectively minimizes flux errors associated with quantization errors. Finally, we test the performance of our method through numerical simulations. We explore the ideal quantization parameters and discuss the implementation details of this new approach.

2 Theory

2.1 Derivation of quantized eddy accumulation

In the following, we derive a general equation for conditional sampling flux measurement techniques and show how relaxed eddy accumulation (REA) can be formulated as a special case of this equation.

We consider the flux F ($\text{mol m}^{-2} \text{s}^{-1}$) of an atmospheric constituent c , such as CO_2 , as

$$F = \overline{w\bar{c}} = \overline{w'c'} + \bar{w}\bar{c} \quad (1)$$

Here, w represents the vertical wind velocity (m s^{-1}), and c represents the molar density (mol m^{-3}) of the scalar in question. Overlines indicate averaging that follows Reynolds averaging rules, while the primes indicate deviations from the mean. The previous equation can be derived from conservation laws. For a

detailed discussion of surface flux equations, refer to Finnigan et al. [2003] and Foken et al. [2012]. The definition in Eq. 1 is chosen as eddy accumulation methods measure, by definition, the term $\overline{w\bar{c}}$. However, similar to eddy covariance (EC) measurements, the term $\overline{w\bar{c}}$ is typically biased due to inaccuracies in w [Emad and Siebicke, 2023a]. The estimation of the physical \bar{w} associated with non-turbulent transport is still relevant, as in EC measurements, and depends on the used concentration index [Kowalski, 2017, Kowalski et al., 2021]. However, these aspects do not affect our subsequent analysis.

We apply a quantizer function $Q(w)$ to restrict the possible values of w to a finite, discrete set. To ensure high flexibility and ease of implementation in flux measurements, we consider a non-uniform quantizer with three levels: $(-w_f, 0, +w_f)$. These quantization levels do not need to be uniformly spaced. The quantizer function compares measured wind speeds with a quantization threshold, denoted as q_t . If the measured magnitude of wind speed exceeds this threshold, the quantized value of w becomes the full-scale value w_f or $-w_f$ depending on the direction of w . The quantizer function is expressed as

$$Q(w, q_t, w_f) = \begin{cases} \text{sign}(w) w_f, & \text{if } |w| > q_t \\ 0, & \text{if } |w| \leq q_t \end{cases} \quad (2)$$

We define the quantization error ε as the difference between the true value of w and the quantized output w_q such that

$$\varepsilon = w - w_q. \quad (3)$$

Consequently, the flux can be written as the sum of the flux of the quantized wind and the flux of the quantization error

$$\overline{w\bar{c}} = \overline{c(w_q + \varepsilon)} = \overline{w_q\bar{c}} + \overline{\varepsilon\bar{c}}. \quad (4)$$

We are more interested in the term $\overline{w'\bar{c}'}$, we rearrange the previous equation and decompose w_q and ε into mean and fluctuating components. We obtain

$$\overline{w'\bar{c}'} = \overline{w_q\bar{c}} + \overline{\varepsilon'\bar{c}'} - \overline{w_q\bar{c}} \quad (5)$$

We express the flux of quantized wind, $\overline{w_q\bar{c}}$, using the law of total expectation as the expectation of the conditional mean of the random variable $c \times w_q$ partitioned on the variable I . The variable I divides the probability space of $w_q c$ into distinct, non-overlapping partitions $\{I_1, I_2, \dots, I_k\}$. The expectation of $\overline{c w_q | I}$ is calculated as a sum over these partitions, each weighted by the probability of its occurrence. Thus, Equation 5 is written as

$$\overline{w'\bar{c}'} = \sum_{j=1}^k \overline{c_{I_j} w_{qI_j}} \times P(I_j) + \overline{\varepsilon'\bar{c}'} - \overline{w_q\bar{c}} \quad (6)$$

The usefulness of this formulation becomes evident when we consider that for a any quantization level, $\overline{w_q\bar{c}} = \overline{w_q\bar{c}}$. This allows us to obtain the covariance term $\overline{w_q\bar{c}}$ directly from measurements of the mean $\overline{c_{I_j}}$ in different partitions instead of

requiring the high-frequency measurements of c . Additionally, the realization of $\overline{w_{qI_j} c_{I_j}}$ for a given I_j by air accumulation is more straightforward as it requires no proportional control of the airflow.

If we consider a simple partitioning scheme based on the direction of vertical wind velocity, $I = \text{sign}(w)$, and choose σ_w , the standard deviation of w , as the full-scale value for our quantizer, we obtain the quantized time series w_q with the same length as w but with values that can be either $-\sigma_w$ or σ_w . The flux can then be obtained from Eq. 6 as

$$\overline{w'\bar{c}'} = \sigma_w \overline{c^\uparrow} \frac{n^\uparrow}{n} - \sigma_w \overline{c^\downarrow} \frac{n^\downarrow}{n} - \bar{c} \sigma_w \frac{n^\uparrow - n^\downarrow}{n} + \overline{c'\bar{c}'} \quad (7)$$

We notice that when $n^\uparrow = n^\downarrow$, the previous equation is reduced to the familiar formula

$$\overline{w'\bar{c}'} = \frac{1}{2} \sigma_w \Delta C + \overline{c'\bar{c}'} \quad (8)$$

Comparing this simplified formula to the common equation used to define REA flux reveals that the measured quantities in REA correspond directly to the flux resulting from quantized wind speed, specifically $\sigma_w \Delta C = 2 \overline{w_q'\bar{c}'}$. This comparison highlights that REA ignores the flux associated with the quantization error, $\overline{c'\bar{c}'}$, and estimates the true flux from the quantized flux through the empirical parameter β which is effectively the ratio of the true flux to the quantized flux $\beta = \overline{w'\bar{c}'} / (2 \overline{w_q'\bar{c}'})$.

Equation 7 highlights two fundamental limitations in conventional REA methods. First, they neglect the flux component $\overline{\varepsilon'\bar{c}'}$, and instead estimate its value empirically through the parameter β . Second, the quantization does not preserve the mean wind, $\overline{w_q} \neq \bar{w}$, as this would require $n^\uparrow = n^\downarrow$ which is rarely the case. The nonzero $\overline{w_q}$ leads to a biased flux estimate due to the inability to account for the term $\bar{c} \overline{w_q}$ when using a quantization threshold different from zero (a deadband).

This raises the question of whether using more optimal quantization —by selecting better values for the quantization threshold and full-scale value— could lead to improved estimates of the term $\overline{\varepsilon'\bar{c}'}$. Essentially, the aim of varying β parameterization schemes and adjusting deadbands in REA is to address this specific issue. However, these modifications had achieved limited success.

Rather than improving the estimates of the term $\overline{\varepsilon'\bar{c}'}$, we propose to reduce its value to zero by randomizing the quantization error to eliminate its correlation with the scalar concentration. The randomization can be achieved by adding pseudorandom noise to the wind signal. The added noise is formed from past errors through a feedback loop, a process known as error diffusion. A simple form of error diffusion can be expressed as

$$w_q[n] = Q(w[n] - \varepsilon[n-1]), \quad (9)$$

where $w_q[n]$ is the quantized wind speed at time n , $w[n]$ is the measured wind speed, and $\varepsilon[n-1]$ is the quantization error at the previous time step. This approach effectively eliminates the

correlation between the quantization error and the scalar concentration. Therefore, making the measured flux of quantized wind speed, $\overline{w'_q c'}$, equal to the true flux, which allows to obtain direct flux estimates and eliminates the need for the parameter β .

The addition of noise to improve the quality of quantized signals is a well-known technique in signal processing. Error diffusion is commonly employed in image and audio processing applications to enhance the perceptual quality of quantized signals [Knox, 1999, Kite et al., 1997, Escbbach et al., 2003]. We refer to this variant of eddy accumulation as quantized eddy accumulation (QEA) with error diffusion.

2.2 Analysis of error diffusion

We are interested in analyzing the signal and noise-shaping behavior of error diffusion. We consider quantization and error diffusion as a system that takes an input signal $x(n)$ and produces an output signal $y(n)$, where the input signal is the vertical wind velocity and the output signal is the quantized wind velocity. We first show that error diffusion acts as a high-pass filter on the noise, then we discuss the optimal choice of the error diffusion filter.

The first step of quantization and error diffusion is forming the modified input. This is achieved by subtracting "diffused" past error terms from the input. We write a similar, but more general form of Eq. 9 as

$$u(n) = x(n) - \sum_{k \in \mathcal{O}} h(k) e(n - k). \quad (10)$$

Here, $u(n)$ represents the modified input, $x(n)$ corresponds to the input of the system such as vertical wind velocity. The diffusion of past errors $e(n - k)$ is represented by the linear weighting filter, denoted as h . \mathcal{O} is the causal support set that does not include 0, signifying that it only includes past errors.

In the second step, the output of the system $y(n)$ is calculated by applying the quantization function $Q(\cdot)$ to the modified input.

$$y(n) = Q(u(n)), \quad (11)$$

In our use case, the output of the system will be the quantized vertical wind velocity that had past errors integrated into it. The quantizer error $e(n)$ is defined as the difference between the output, $y(n)$, and the modified input

$$e(n) = y(n) - u(n), \quad (12)$$

note that this is different from the quantization error defined earlier. We substitute Eq. 10 into Eq. 12, we find

$$e(n) = y(n) - x(n) + \sum_{k \in \mathcal{O}} h(k) e(n - k) \quad (13)$$

The previous equation highlights the recursive character of error diffusion, where the error at any given moment in time depends on the entire history. To analyze this relation in the frequency domain, we apply the z -transform which converts discrete-time signals from the time domain into the z -domain [Smith, 2007].

After applying the z -transform and rearranging, we can write Eq. 13 as

$$Y(z) - X(z) = (1 - H(z))E(z). \quad (14)$$

Here, $H(z) = \sum h(k)z^{-k}$, is the filter applied to past errors in the frequency domain. The variable z is a complex exponential reflecting the frequency components of the signal and is defined as $z = \exp(j\omega T)$, where ω is the angular frequency in radians per sample, and T is the sampling interval. Considering that $G(z) = Y(z) - X(z)$ represents the total quantization error, which corresponds to the output of the noise transfer function, we find the transfer function describing the frequency shaping of the noise by rearranging the previous equation to be

$$\text{NTF}(z) = \frac{G(z)}{E(z)} = 1 - H(z) \quad (15)$$

Equation 14 indicates that the total quantization error ε , defined as the difference between the system output and its input, consists of two errors: one is a filtered version of the other. The first error component is the quantizer error $E(z)$, which we defined as the difference between the output and the modified input. The second error component is the filtered quantizer error, which we call the diffusion error $E(z)H(z)$.

Error diffusion can be viewed as an error minimization process. It aims to reduce the difference between the input and the output by adjusting the weights of a linear filter [Escbbach et al., 2003]. In our specific application, our primary interest lies not in minimizing the quantization error itself, but rather in minimizing its correlation with the scalar concentration c , therefore, we want to choose $H(z)$ such that the filtered output $H(z)E(z)$ is as close as possible to $E(z)$. Given that $H(z)$ has to be causal, we find the unit delay filter, denoted as $H(z) = z^{-1}$, as the optimal solution for minimizing the correlation of the quantization error with the scalar. The unit delay filter allows all frequencies to pass unattenuated and introduces a linear phase shift, which, in this case, results in a one-sample delay of the input. This means that the error from the previous time step is added in its entirety. The rationale for this choice is that $e(n)$ is not completely random; instead it has an autocorrelation structure due to the recursive nature of error diffusion. Therefore, the closest version of $e(n)$ that can be achieved using a causal filter is a one-sample-delayed version of itself. The previous equation with $H(z)$ as the unit delay filter indicates that the mean of the output equals the mean of the input because the filter coefficients sum to one; therefore, at zero frequency, $H(1) = 1$.

To investigate the behavior of flux errors, we can express the quantization error covariance term in the time domain as:

$$\overline{\varepsilon' c'} = \overline{e' c'} - \overline{(h * e)' c'}, \quad (16)$$

where $*$ denotes convolution. Given that diffusion error represents a one-sample delayed version of $e(n)$ and based on the definition of the cross-covariance function between e and c , denoted as $R_{ec}(n)$, we can express the error covariance as

$$\overline{\varepsilon' c'} = R_{ec}(0) - R_{ec}(1) \quad (17)$$

Typically, e is assumed to be white noise for a uniform quantizer [Kite et al., 2000]. However, for a non-uniform quantizer, e exhibits correlation with w and c . To address this issue, we can apply error diffusion per wind direction, effectively treating the updraft and downdraft as separate signals. This approach enables non-uniform quantization without introducing correlation, which offers more flexibility in choosing quantization thresholds and full-scale values. Modeling the quantizer directly is challenging due to its nonlinearity, which complicates the characterization of the cross-correlation function R_{ec} , especially when applying diffusion per wind direction. However, e is expected to exhibit some autocorrelation structure due to the recursive nature of error diffusion. This autocorrelation further contributes to minimizing the flux error in Eq. 17. The experimental simulation results in the results section confirm this analysis.

2.3 Calculation of QEA fluxes

We show here how the flux is calculated in QEA for the simple case of partitioning based on the sign of w . In this case, the quantized flux in equation 6 becomes

$$\overline{w_q c} = \overline{c^\uparrow w_q^\uparrow} p^\uparrow + \overline{c^\downarrow w_q^\downarrow} p^\downarrow, \quad (18)$$

where the arrows indicate updraft and downdraft, and p is the probability of wind direction being in the given direction. After the end of the averaging interval, typically spanning 30 minutes to 1 hour, the flux $\overline{w'c'}$ is obtained from Eq. 6 as

$$F_{\text{total}} = \overline{w'c'} = \overline{c^\uparrow} \overline{w_q^\uparrow} \frac{n_q^\uparrow}{n} + \overline{c^\downarrow} \overline{w_q^\downarrow} \frac{n_q^\downarrow}{n} - \overline{c} \overline{w_q} + \overline{\varepsilon' c'}, \quad (19)$$

where $\overline{c^\uparrow}$ and $\overline{c^\downarrow}$ represent the average scalar concentrations in the updraft and downdraft reservoirs, while n_q^\uparrow and n_q^\downarrow indicate the counts of occurrences with the quantized wind direction as updraft and downdraft, respectively. The variable n represents the total number of vertical wind velocity samples within the averaging interval.

Equation 19 includes the term $\overline{c} \overline{w_q}$, which requires knowledge of the average scalar concentration \overline{c} within the averaging interval. Estimating this term is a common challenge in eddy accumulation methods and arises due to the presence of a biased non-vanishing mean vertical wind velocity. The root of this issue is that samples are accumulated in real time without full knowledge of wind statistics throughout the averaging interval, making it impossible to ensure that \overline{w} is zero. Solutions to this problem typically involve estimating \overline{c} from available measurements and the properties of atmospheric transport [Emad and Siebicke, 2023a]. We note that for QEA with a zero quantization threshold, \overline{c} can be calculated directly from the measurements of $\overline{c^\uparrow}$ and $\overline{c^\downarrow}$. To accommodate the estimation of \overline{c} from available measurements, we express the total flux, F_{total} as the product of the base flux, F_1 , a correction factor, $A_{\overline{w}}$, to

account for non-zero mean wind velocity, and the quantization error covariance component F_{error}

$$F_{\text{total}} = F_1 \cdot A_{\overline{w}} + F_{\text{error}} \quad (20)$$

The base flux, F_1 , is derived from measurable quantities

$$F_1 = \overline{c^\uparrow} \overline{w_q^\uparrow} \frac{n_q^\uparrow}{n} + \overline{c^\downarrow} \overline{w_q^\downarrow} \frac{n_q^\downarrow}{n} - \left(\overline{c^\uparrow} \frac{n_q^\uparrow}{n_q} + \overline{c^\downarrow} \frac{n_q^\downarrow}{n_q} \right) \overline{w_q}, \quad (21)$$

where n_q is the count of occurrences where $w_q \neq 0$ and n is the total sample count in the averaging interval.

The correction factor, $A_{\overline{w}}$, adjusts for the discrepancy between the measured average concentration, \overline{c} , and its true value, with higher wind variability leading to reduced error, and can be estimated as

$$A_{\overline{w}} = \frac{1}{1 - \alpha_c \frac{\overline{w_q}}{|w_q|}}, \quad (22)$$

where α_c is the atmospheric transport asymmetry coefficient defined as the ratio $\overline{c' |w'_q|} / \overline{c' w'_q}$ and accounts for the correlation when estimating \overline{c} from $\overline{c |w_q|}$. The value of α_c can be estimated analytically or empirically [Emad and Siebicke, 2023a]. Lastly, F_{error} represents the error in the flux due to the quantization error previously discussed, typically less than 0.1% of the flux. If the units of measured $\overline{c^\uparrow}$ and $\overline{c^\downarrow}$ are dry mole fractions $\text{mole} \cdot \text{mole}^{-1}$, we divide the resulting flux by the molar volume of dry air V_{md} ($\text{m}^3 \cdot \text{mole}^{-1}$) to obtain the flux density in units of $\text{mol} \cdot \text{m}^{-2} \cdot \text{s}^{-1}$. An implementation and examples of flux calculation for this method are provided in the supplementary material.

3 Methods

3.1 Simulation data and parameters

We used a high-frequency dataset of eddy covariance (EC) measurements collected from two contrasting ecosystems as input for our simulation. The first is an ideal flat agricultural field at the Thünen Institute in Braunschweig, Germany (52.30° N, 10.45° E), where wind measurements were obtained using a sonic anemometer (uSonic-3 Class A, Metek GmbH, Elmshorn, Germany) and an open-path infrared gas analyzer (LI-7500A, LI-COR Biosciences Lincoln, NE, USA) at 10 Hz sampling frequency. Data from this site covered two periods in 2020, from June 1 to July 15 and from October 1 to November 10, resulting in 3,146 30-minute averaging intervals across 65 days. The second site is an old-growth forest in the Hainich National Park (ICOS DE-Hai) in Thuringia, Germany (51.08° N, 10.45° E). Here, measurements were taken using a 3D sonic anemometer (Gill-HS, Gill Instruments Limited, Hampshire, UK) and an enclosed-path infrared gas analyzer (LI-7200, LI-COR Biosciences Lincoln, NE, USA). Data used at the Hainich site covered two periods in 2022, from June 1 to June 31 and from August 11 to September 15, with a total of 3,490 30-minute

averaging intervals over 72 days. Further details on the sites and instrumentation specifications can be found in [Emad and Siebicke, 2023b] and [Knohl et al., 2003] respectively.

Using this dataset, we simulated flux measurements for three variables: CO_2 , H_2O , and air temperature measured with a sonic anemometer (θ). Our simulation included the newly developed quantized eddy accumulation and six conventional relaxed eddy accumulation variants, serving as baselines for performance benchmarking under the same constraints. Fluxes for the different methods were calculated based on 30-minute averaging intervals, and basic quality controls were applied to the calculated fluxes. Quality control measures included flagging periods where stationarity tests failed or where the friction velocity was below 0.1 m s^{-1} [Foken et al., 2005].

The simulation aimed to assess the performance of the QEA method with error diffusion and determine its optimal parameters for various key objectives. The performance evaluation aimed to quantify flux errors associated with these methods, relative to the reference eddy covariance method. This assessment included both systematic and random components of error. Here, we consider systematic errors to be those correlated with the measured flux value. Flux errors are defined as the difference between the measured flux using a given method and the reference eddy covariance flux. To provide a relative measure of the systematic error that works across different scalars, we chose the slope of a linear regression of the flux error against the flux value as a metric to quantify systematic errors.

Random errors, in contrast, are not correlated with the magnitude of the flux, although their variance may still show a correlation with the flux value. The impact of random errors is generally less severe since they tend to diminish with averaging. The influence of random errors can be estimated by calculating the standard deviation of the errors around the measured flux value, providing a measure of the method’s uncertainty. However, as we aim to establish general relative measures for the uncertainty of the compared methods rather than specifying values for a given scalar, We define the normalized error E_{norm} as the ratio of the flux error to the product of the standard deviations of the vertical wind velocity and the scalar

$$E_{\text{norm}} = \frac{F_{\text{meas}} - F_{\text{ref}}}{\sigma_w \sigma_c}, \quad (23)$$

where F_{meas} is the measured flux for a certain method, F_{ref} is the reference eddy covariance flux. This definition essentially transfers the error to be expressed as error in the correlation coefficient ρ_{wc} . The standard deviation of the normalized error can be used as a non-dimensional measure of the uncertainty of the method

$$u_{\text{nd}} = \sqrt{\text{Var}(E_{\text{norm}})} \quad (24)$$

The usefulness of this expression is that it facilitates comparisons of uncertainty across different scalars as the correlation coefficient is seen as an independent measure of atmospheric transport. Additionally, it enables the calculation of the relative uncertainty of the flux when divided by the correlation coefficient ρ_{wc} . For example, a non-dimensional uncertainty of 0.01 implies that, if $\rho_{wc} = 0.4$, there is a 95% probability that the flux will be within $\pm 5\%$ of the measured value, assuming a normal distribution of the error.

While we use EC fluxes as our reference, it is important to note that EC fluxes have limitations, particularly during low turbulence or over complex terrain. Eddy accumulation methods are designed to address issues of sensor response time and signal strength, aiming to match EC flux measurements when using slow-response sensors. However, these methods cannot solve fundamental problems unrelated to sensor limitations, such as violations of EC assumptions. We therefore use EC as a reference to evaluate the performance of the eddy accumulation methods.

Choosing a method for estimating or parametrizing β poses a common challenge for REA methods, as there are no clear recommendations that universally apply across all sites and atmospheric conditions. We chose six methods to estimate β as recommended by recent work on REA [Vogl et al., 2021]. These treatments included the commonly used β calculated from sonic temperature $\beta_{ts} = \overline{w'\theta'}/(\Delta\theta\sigma_w)$, a constant β estimated as the median of β calculated from air temperature $\beta_{ts-\text{median}}$, and β calculated from vertical wind velocity statistics as $\beta_w = \sigma_w/\Delta w$ following Baker [2000]. Additionally, we used for each of the previous methods two dynamic linear deadband settings, namely, $0.5\sigma_w$ and $0.9\sigma_w$. The β values calculated using these methods were subsequently used to compute REA fluxes through the equation $F_{\text{REA}} = \beta\sigma_w\Delta C$. Each method is identified by combining the β estimation technique with the chosen deadband setting, such as REA (db 0.5σ) $\beta_{ts-\text{median}}$.

Quantized eddy accumulation with error diffusion was simulated with a wide range of parameters. The algorithm used to simulate QEA with error diffusion is detailed in Section 4.4. For performance comparison with REA variants, we selected the parameter pair ($q_t = 2.4\sigma_w$, $w_f = 4\sigma_w$). The full code of the simulation and the analysis are available at Emad [2024a].

4 Results and Discussion

4.1 Quantized eddy accumulation with error diffusion

We have developed a general framework for conditional sampling methods in Eq. 6 by combining quantization of vertical wind speed with conditional sampling. Conventional relaxed eddy accumulation method was shown to be a special case of this framework when setting the conditioning variable I to $\text{sign}(w)$ and quantizing wind speed into two discrete levels that correspond to the standard deviation of the wind $-\sigma_w$ and $+\sigma_w$ as seen in Eq. 7. The parameter β is found to be fundamentally linked to an unaccounted flux term that is carried with quantization errors arising from non-optimal quantization. This connection explains the difficulty in estimating β as it involves estimating a covariance term based on the conditional mean of scalar concentration and wind statistics.

We proposed to use error diffusion to eliminate the covariance term $\overline{e'c'}$ by adding pseudorandom noise to w in a feedback loop. Eliminating this term makes the quantized flux $\overline{w_q c}$ equal to the true flux $\overline{w' c'}$ and eliminates the need for the empirical coefficient β . The error diffusion algorithm is seen as an error minimization mechanism, as pseudorandom noise is introduced

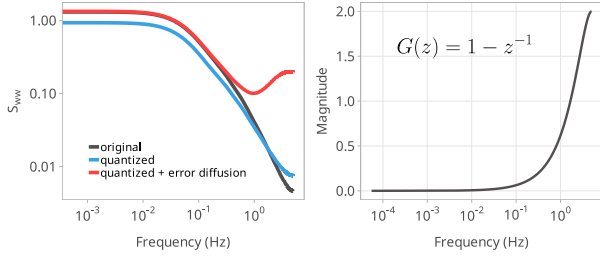


Figure 1: Spectral analysis of error diffusion. (a) Normalized averaged power spectral density of vertical wind velocity for a typical 30-minute interval. The ‘original’ curve represents the original spectrum, while the ‘quantized’ and ‘quantized + error diffusion’ curves illustrate the effects of quantization and subsequent error diffusion on the signal. The noise shaping behavior is demonstrated by the deviation of ‘quantized + error diffusion’ spectrum from the ‘original’, particularly in the higher frequency range. (b) Magnitude response of the noise transfer function, displaying the high-pass characteristics of the $G(z) = 1 - z^{-1}$ filter, with a steady increase in magnitude with frequency, demonstrating the noise shaping capability. The displayed spectra are averaged from 50 samples taken from random 30-minute intervals that meet the quality standard $|\rho_{wc}| > 0.3$ and $\sigma_w > 0.4$.

into the signal to reduce the error correlation with the scalar. We found that a simple variant of error diffusion where the complete quantization error is added to the next sample is optimal for minimizing the correlation between the quantization error and the scalar concentration. This corresponds to using the unit delay filter $H(z) = z^{-1}$ in Eq. 14.

QEA with error diffusion offers the advantage of increasing the difference between mean accumulated concentrations in updraft and downdraft reservoirs ΔC , thereby improving the signal-to-noise ratio. The quantization of wind with a threshold larger than zero, similar to employing a deadband in REA, serves the purpose of filtering out low wind speeds that are associated with smaller scalar fluctuations. This concentration enhancement is especially useful when measuring atmospheric constituents with low flux. Importantly, this concentration enhancement does not introduce additional uncertainty to the flux as error diffusion performance is largely independent of the quantization threshold as is shown in Fig. 4.

The analysis of error diffusion in the z -domain reveals that the quantizer noise is pushed towards the higher end of the spectrum, as shown in Fig. 1. Consequently, the spectrum of the quantization error exhibits characteristics resembling blue noise, with a significant concentration of power in the high-frequency range. When we consider the unit delay filter $1/z$ for the error diffusion filter. The noise transfer function in Eq. 15 becomes $\text{NTF}(z) = 1 - z^{-1}$. $\text{NTF}(z)$ exhibits a frequency response that amplifies higher frequencies, as indicated by the magnitude plot in Fig. 1. The gain increases linearly with frequency, peaking at twice the input signal’s amplitude at the Nyquist frequency. This characteristic introduces additional energy into the system at higher frequencies, effectively shaping

the noise spectrum which is beneficial in flux measurements as the noise at higher frequencies is typically more tolerable.

Error diffusion is found to be mean preserving; the mean output signal equals the mean of the input as the filter coefficients sum to unity. Furthermore, our analysis shows that the total quantization error comprises two components, one of which is a filtered version of the other as shown in Eq. 14.

Flux error resulting from quantization and error diffusion is mainly attributed to the residual spurious correlation between the quantization error and the scalar concentration $\varepsilon' c'$. The flux error is found to be equal to the difference between the values of the cross-covariance function $R_{ec}(n)$ evaluated at indices 0 and 1, as shown in Eq. 17. This implies that a larger auto-correlation of $e(n)$ corresponds to a smaller error, as a one-sample delayed error will have a stronger correlation with the current $e(n)$. The variant of error diffusion proposed in this study diffuses the error per wind direction, ensuring that the error $e(n)$ remains uncorrelated with the scalar concentration $c(n)$ even when a non-uniform quantizer is used. This variant allows for a more flexible choice of quantization parameters, which is very useful for practical implementations, as will be shown in the Section 4.4.

4.2 Performance evaluation of error diffusion

A simulation-based assessment of the newly developed error diffusion algorithm indicates a substantial enhancement in accuracy and reduction in uncertainty over conventional relaxed eddy accumulation methods as shown in Fig. 2 and Fig. 3.

We evaluated the performance of the QEA method using high-frequency eddy covariance data for three scalars (CO_2 , H_2O , and θ), across two contrasting ecosystems over 18 weeks. We distinguished between systematic errors, which correlate with the flux values, and random errors, which do not correlate and are expected to diminish with time averaging. To standardize error metrics across different scalars, we normalized the error by the product of σ_w and σ_c , as shown in Eq. 23, and defined the non-dimensional uncertainty as the standard deviation of this normalized error.

The analysis of the simulation results revealed no systematic biases in QEA fluxes with error diffusion for all tested scalars, sites, and atmospheric conditions. The slopes of the error against reference flux values—were consistently below 0.1%, significantly lower than the average 5% bias found with the commonly used REA methods, as shown in Fig. 2.

The QEA method have consistently demonstrated minimal random errors, with a non-dimensional uncertainty below 0.004 for all scalars, significantly lower than the 0.05 observed with the best-performing REA variant as shown in Fig. 3. The uncertainty of QEA is smaller than the theoretical uncertainty expected from the correlation coefficient of two random samples, calculated as $\sigma_r = (1 - r^2)/\sqrt{n - 3}$ [Gnamb, 2022, Bonett and Wright, 2000] and shown as red lines on Fig. 3. This can be attributed to the auto-correlation of the quantizer error that makes the difference $R_{ec}(0) - R_{ec}(1)$ very small.

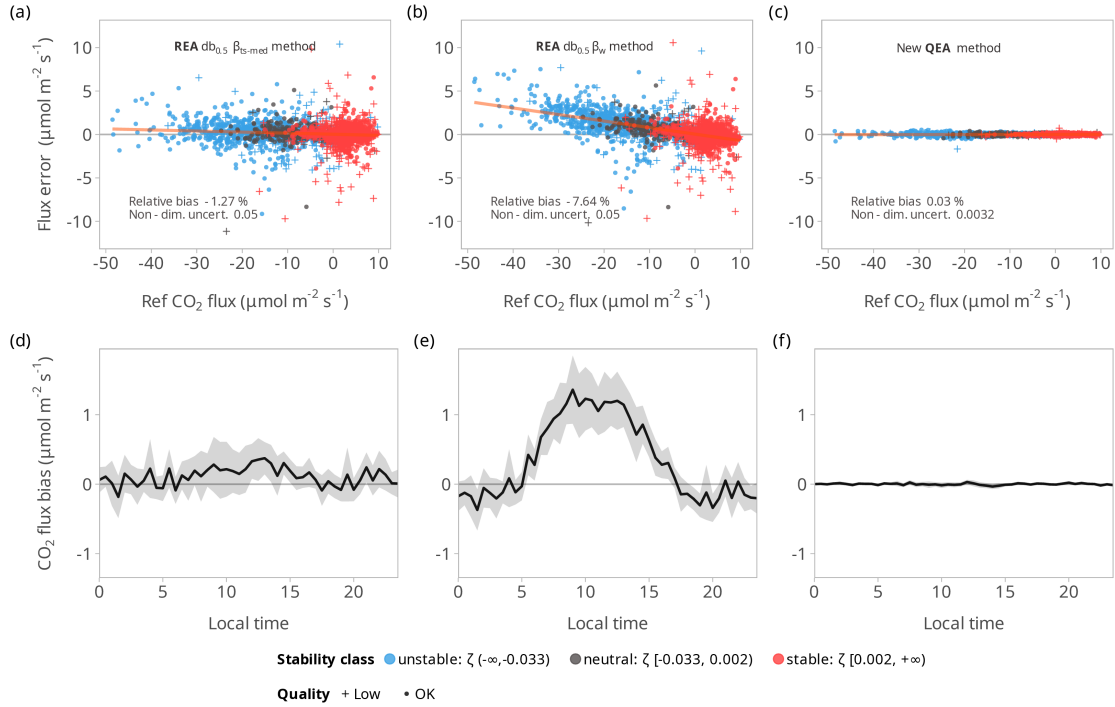


Figure 2: Performance evaluation of quantized eddy accumulation. (a)-(c) Scatter plots displaying the dependence of flux errors on the reference flux for CO₂ for two established relaxed eddy accumulation (REA) variants ($\beta_{0.5\text{-med}}$ and β_w) versus the novel quantized eddy accumulation (QEA) method with error diffusion. Flux errors for CO₂ are calculated as the difference relative to eddy covariance reference flux measurements, differentiated by atmospheric stability classes: unstable (blue), neutral (gray), and stable (red) and two flux quality classes (point shape). These categories illustrate the error’s sensitivity to atmospheric stability. Reported relative bias is the slope of the error versus the reference value. Reported non-dimensional uncertainty is defined as the standard deviation of flux errors normalized by $\sigma_w \sigma_c$ for the entire dataset. (d)-(f) Diurnal mean of CO₂ flux errors for each method, with a 95% confidence interval shaded region generated via bootstrapping. This demonstrates the temporal variability of biases throughout the day, and demonstrates the QEA method’s robustness, as reflected in its consistent closeness to the reference eddy covariance flux. The data shown are for the Braunschweig station. Reported error metrics and diurnal flux errors are for the quality-filtered dataset. For QEA, a quantization threshold $q_t = 2.4\sigma_w$ and a full scale value $w_f = 4\sigma_w$ were used.

Importantly, the accuracy of QEA was not influenced by the time of day, atmospheric stability, or flux quality metrics, unlike the REA methods, as shown in Fig. 2. These findings, along with several other error metrics, are summarized in Table 1 and Table 2, demonstrating that QEA outperforms REA across all examined conditions and metrics. The relative improvement ratio of QEA over REA variants reported in Table 2 shows wide variation across the different REA methods and scalars. However, QEA has a consistent improvement over all REA methods and scalars with the error slope showing over 100-fold improvement compared to the best-performing REA variant and up to 1000-fold improvement for some variants and scalars. Additional figures are provided in the supplementary material showing more detailed comparisons of the performance of QEA and REA methods across different scalars and stations.

4.3 Optimal quantization parameters

QEA with error diffusion has two parameters: the quantization threshold q_t and the quantized full-scale value w_f . The

choice of these parameters allows for minimizing the flux error, maximizing the concentration difference ΔC in accumulation reservoirs, reducing the error due to nonzero mean vertical wind velocity, and controlling the switching rates of the sampling valves.

The main objective of the evaluation presented here was to establish optimal ranges for the quantizer parameters that optimize for the above goals. These goals were assessed through numerical simulations for three different scalars over a broad range of parameters. Simulation results indicated that, for all scalars, the flux error remained consistently low across a wide range of q_t and w_f combinations, as shown in Fig. 4. Generally, the error stayed below 1% for almost any combination of parameters, provided that the full-scale value was greater than $2.7\sigma_w$. Notably, a large number of parameter combinations resulted in errors smaller than 0.1%. The random errors showed similar trends, with the non-dimensional uncertainty typically being lower for parameter combinations that minimized systematic errors. The error diffusion algorithm variant used in this simulation diffuses quantization errors per wind direction. This

Table 1: Comparative performance evaluation of quantized eddy accumulation (QEA) with error diffusion versus conventional relaxed eddy accumulation (REA) methods for CO₂, H₂O, and air temperature (θ) fluxes. Performance metrics include error slope (dimensionless), error intercept (units of flux), non-dimensional uncertainty, and root mean square error (RMSE, units of flux). Error metrics are calculated as averages for two contrasting ecosystems and obtained from a simulation using a high-frequency eddy covariance dataset. For QEA, a quantization threshold $q_t = 2.4\sigma_w$ and a full scale value $w_f = 4\sigma_w$ were used.

Method	Scalar	Error slope	Error intercept	Nondim. uncertainty	RMSE
QEA with error diffusion	CO ₂	1.61×10^{-4}	4.19×10^{-4}	2.66×10^{-3}	0.065
	H ₂ O	7.73×10^{-5}	1.02×10^{-4}	2.08×10^{-3}	8.90×10^{-3}
	θ	6.85×10^{-6}	-1.09×10^{-5}	3.21×10^{-3}	3.16×10^{-4}
REA β_{ts}	CO ₂	-0.016	0.032	0.430	6.891
	H ₂ O	-0.048	-4.19×10^{-3}	0.692	1.204
REA (db 0.5 σ) β_{ts} -median	CO ₂	-0.021	0.020	0.058	1.256
	H ₂ O	-0.040	5.28×10^{-3}	0.056	0.169
REA (db 0.9 σ) β_w	CO ₂	0.018	-0.022	0.056	1.165
	H ₂ O	0.026	-5.99×10^{-3}	0.053	0.154
	θ	0.017	1.21×10^{-4}	0.060	5.10×10^{-3}
REA (db 0.5 σ) β_w	CO ₂	-0.095	0.032	0.059	1.809
	H ₂ O	-0.120	0.013	0.056	0.243
	θ	-0.075	-1.64×10^{-4}	0.062	8.54×10^{-3}

Table 2: Average improvement ratio of quantized eddy accumulation (QEA) method over relaxed eddy accumulation (REA) variants. The table shows the mean enhancement of QEA over REA variants for each error metric. The improvement ratio for each error metric is calculated by dividing the average metric value for REA across three scalars and two stations by the corresponding average value for QEA. Ratios larger than one indicate areas where QEA shows significant advantages

Method	RMSE	Error intercept	Error slope	Nondim. uncertainty
REA (db 0.9 σ) β_{ts}	264	1070	133	499
REA (db 0.9 σ) β_{ts} -median	25	185	334	23
REA β_{ts}	173	200	546	219
REA (db 0.9 σ) β_w	21	68	401	21
REA (db 0.5 σ) β_{ts} -median	28	67	537	23
REA (db 0.5 σ) β_{ts}	947	1788	1290	618
REA (db 0.5 σ) β_w	41	108	2161	26

variant was found to be more effective in reducing errors and offers greater flexibility in the choice of quantization parameters, as will be shown in Section 4.4.

Adjusting the quantization threshold can improve the signal-to-noise ratio by increasing the difference in concentration ΔC between the two accumulation reservoirs, as illustrated in Fig. 5. The key driving factor in increasing ΔC is the ratio between the quantization threshold and the quantized full-scale value, referred to as the scaled quantization threshold. Values greater than 0.5 can increase ΔC by up to 150%, akin to introducing a deadband in REA measurements, which leads to the selective accumulation of eddies with concentrations further away from the mean. However, unlike REA where increasing the deadband is accompanied by an increase in flux uncertainty [Onclay et al., 1993, Pattey et al., 1993], selecting a higher quantization threshold to increase ΔC does not reduce the accuracy of fluxes measured with QEA as seen from Fig. 4.

Reducing the scaled quantization threshold can help minimize errors related to non-zero mean vertical wind velocity. This reduction coincides with a decrease in ΔC , as shown in Fig. 5. The reduction of errors caused by non-zero mean wind velocity is driven by increased wind variance (and thus, $\overline{|w|}$), which is inversely correlated with flux error magnitude under conditions when the mean wind is not zero [Emad and Siebicke, 2023a]. A scaled quantization threshold below 0.5 is effective in decreasing these errors as shown in Fig. 5. A threshold set to zero can remove the influence of non-zero mean vertical wind velocity entirely, which is a unique advantage of QEA over TEA.

Additionally, adjusting the scaled quantization threshold affects how often sampling valves switch and the accumulated sample volumes. Higher thresholds lead to less frequent switching; for example, with a threshold of 0.5, the updraft and downdraft valves switch on average once per second, as shown in Fig. 6.

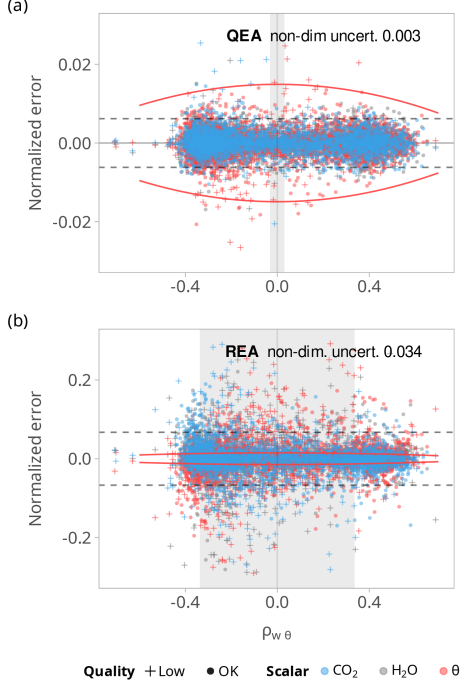


Figure 3: Normalized flux errors for CO₂, H₂O, and air temperature (θ) as a function of the correlation coefficient $\rho_{w\theta}$. Panel (a) shows normalized errors of the quantized eddy accumulation (QEA) method with error diffusion. Panel (b) shows normalized errors of the relaxed eddy accumulation (REA) method using β_w with a deadband of $0.9\sigma_w$. Dashed horizontal lines indicate $\pm 2u$, where u is the non-dimensional uncertainty defined as the standard deviation of the normalized flux errors for the entire dataset. The red lines indicate $\pm 2 \times$ theoretical uncertainty expected from the correlation coefficient of two random samples calculated as $\sigma_r = (1 - r^2) / \sqrt{n - 3}$. The shaded areas represent the range of $\rho_{w\theta}$ where the relative flux uncertainty exceeds 20% of the flux value.

4.4 Implementation of quantized eddy accumulation with error diffusion

Quantized eddy accumulation with error diffusion can be implemented using a varying number of quantization levels and based on different conditioning variables. However, the simplest and most useful implementation is achieved using two reservoirs that accumulate air at a constant flow rate, similar to the requirements of the relaxed eddy accumulation method. Since each quantization level is accumulated in a separate reservoir, no proportional control of the flow is required. We will discuss the specifics of such an implementation here.

The error diffusion algorithm we developed for this implementation is described in Algorithm 1. This implementation requires only a constant airflow rate for air sampling and the channelling of this airflow into either updraft or downdraft reservoirs depending on the sign of quantized wind velocity. In this algorithm, the quantization error is incorporated in a feed-

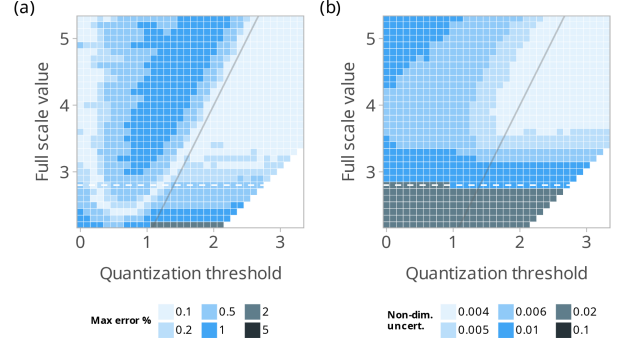


Figure 4: Evaluation of parameter space for systematic bias and uncertainty for CO₂ flux measurements with QEA. Panel (a) shows a heatmap that illustrates the systematic bias, represented by the slope of the linear fit, as a function of the quantization threshold and full-scale value. The color intensity corresponds to the maximum magnitude of the systematic bias in each class. A white dashed line at a full-scale value of 2.7 and a solid line with a slope of 2 indicate the boundaries where systematic biases exceeds 0.2%. Panel (b) presents a heatmap of the maximum non-dimensional uncertainty which indicates error variability. These metrics are calculated based on simulations utilizing the entire dataset for the Braunschweig station.

back loop with the measured vertical wind velocity before it is quantized into three discrete levels corresponding to updraft, downdraft, and no sampling. The quantization error is managed separately for updraft and downdraft. This separation has been found to improve the stability of the flux errors and allows for a wider range of quantization parameters that produce accurate flux estimates.

Algorithm 1 Quantized eddy accumulation with error diffusion

Require: vertical wind speed array w , quantization threshold $q_threshold$, and wind quantized full-scale value w_full

- 1: $N \leftarrow \text{length}(w)$
- 2: $residual_error_up \leftarrow 0$
- 3: $residual_error_down \leftarrow 0$
- 4: **for** $i = 1$ to N **do**
- 5: **if** $w[i] > 0$ **then**
- 6: $w_{mod} \leftarrow w - residual_error_up$
- 7: $w_q[i] \leftarrow Q(w_{mod}, q_threshold, w_full)$
- 8: $residual_error_up \leftarrow w_q[i] - w_{mod}$
- 9: **else**
- 10: $w_{mod} \leftarrow w - residual_error_down$
- 11: $w_q[i] \leftarrow Q(w_{mod}, q_threshold, w_full)$
- 12: $residual_error_down \leftarrow w_q[i] - w_{mod}$
- 13: **end if**
- 14: **end for**
- 15: **return** w_q

The quantized w can take one of three values: $-w_f$, 0 , or w_f , where w_f is the quantized full-scale level. The accumulated volume in each reservoir at the end of the averaging interval is calculated as $V = A n_q T_s$, where A represents a flow scaling

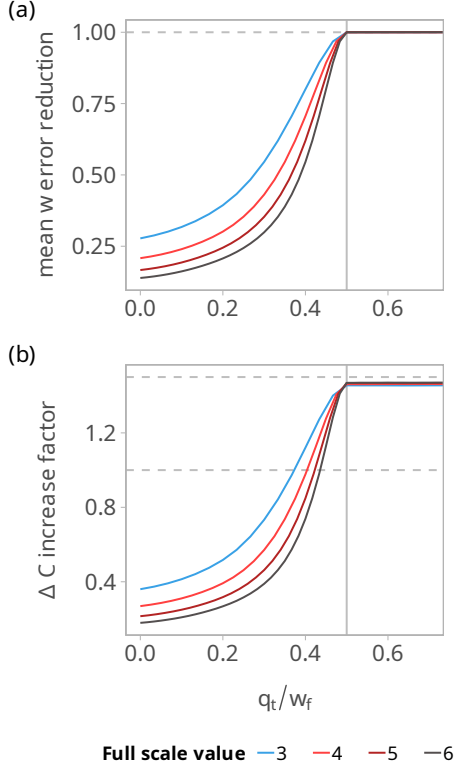


Figure 5: Nonzero mean wind error reduction and ΔC increase of error diffusion. (a) Nonzero mean w error reduction factor against scaled quantization threshold, for full-scale values 3-6, illustrating the impact of quantization on errors associated with nonzero \bar{w} . The reduction factor is calculated as the ratio of the mean of absolute wind velocity $|w|$ to the mean of absolute quantized velocity $|w_q|$. Values below one indicate a reduction in the error. (b) ΔC increase factor, calculated as the slope of a linear fit of ΔC with the given quantization threshold to ΔC with a quantization threshold of zero. Dashed horizontal lines shown at $y=1$ and $y=1.5$. q_t/w_f is the scaled quantization threshold which we defined as the ratio of the quantization threshold to the full-scale value.

factor ($\text{m}^3 \text{s}^{-1}$), n_q is the number of sampling events in the averaging interval, and T_s is the duration of sampling for each event (seconds).

The choice of the quantization threshold (q_t) and the quantizer’s full-scale setting (w_f) plays a crucial role in error control, signal-to-noise ratio enhancement, and reduction of residual mean vertical wind velocity errors. Setting q_t to zero allows for an unbiased estimation of \bar{c} , as it leads to $\overline{c^\uparrow w_q^\uparrow} = \bar{c}^\uparrow \overline{w_q^\uparrow}$. This choice effectively eliminates errors associated with non-vanishing mean wind velocity, which provides an advantage over traditional eddy accumulation methods.

Referring to Fig. 4, we can identify the optimal quantization parameters q_t and w_f . In general, to minimize the errors in fluxes calculated via QEA, it is recommended to use a quan-

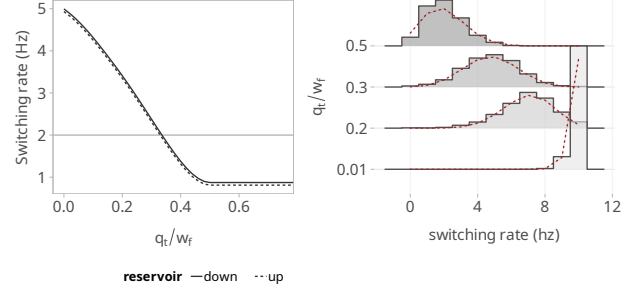


Figure 6: Valve switching dynamics. The left panel illustrates the relationship between the scaled quantization threshold and the average valve switching rate (Hz), distinguishing between reservoirs (‘down’, solid line) and (‘up’, dashed line). The right panel presents histograms of the distribution of valve switch rates (as events per second) for four distinct scaled quantization thresholds simulated from a 30-minute high-frequency wind measurements dataset. Dashed lines indicate the theoretical binomial distribution for the valve switching events per second, with the success probability corresponding to the average valve switching rate and the size parameter as the number of samples taken per second.

tized full-scale value in the range $[4, 5] \sigma_w$ and a quantization threshold in the range 0.55 to 0.85 of the full-scale value. For instance, setting q_t to $2.5\sigma_w$ and the full-scale value to $4\sigma_w$ predicts an average error under 0.1%. Since q_t and w_f depend on the unknown σ_w of the current averaging interval; an estimate from the preceding interval can be used. The heatmap of Fig. 4 illustrates that error diffusion is robust to slight variations in σ_w which supports the use of past data to define the parameters of the current averaging interval. The chosen example parameters suggest nearly a 1.4-fold increase in ΔC and an average valve switching rate of about 2 Hz as seen from figures 5 and 6.

The quantized vertical wind velocity, $\overline{w_q}$, is expected to equal the vertical wind velocity, \bar{w} , because quantization with error diffusion preserves the mean, as demonstrated earlier. The error associated with nonzero $\overline{w_q}$ in QEA can be addressed in three ways: i) Similar to true eddy accumulation methods, an estimate of \bar{c} can be derived from available quantities by averaging c^\uparrow and c^\downarrow with proper weights as shown in Eq. 20. ii) QEA offers an advantage over conventional EA methods. By setting $q_t = 0$, we can calculate \bar{c} from measurements. This, however, may reduce ΔC , as shown in Fig. 5. Still, it can be justified if the analytical instrument is sufficiently accurate. iii) Under stationary conditions, the error associated with a non-zero mean vertical wind velocity (\bar{w}) is limited to the ratio $\bar{w}/|\bar{w}|$ [Emad and Siebicke, 2023a]. Therefore, error diffusion presents a novel opportunity to minimize this error by amplifying the wind’s variance, which subsequently raises the mean absolute wind velocity ($|\bar{w}|$). This strategy effectively mitigates the error related to a non-zero \bar{w} , as demonstrated in Figure 5.

In a typical implementation of the QEA method, real-time vertical wind velocity is acquired and then adjusted through

an online planar fit to align the coordinates to the streamline coordinates, as described in [Siebicke and Emad, 2019]. We recommend subtracting the mean wind of the previous interval (differencing) to minimize residual \bar{w} and achieve a more symmetric distribution of \bar{w} around zero. Subsequently, the wind speed is modified using the previous quantization error and then quantized using Eq. 2 according to Algorithm 1. If the quantized w is non-zero, the flow is directed into the corresponding reservoir. It is important to emphasize that the requirement for flow consistency applies only within each averaging interval and reservoir. Therefore, variations in flow are permissible between updraft and downdraft and across different averaging intervals.

The implementation of the new QEA method with error diffusion presents several critical technical challenges. A key challenge is the need for fast-switching valves, which are essential for directing the flow between the two accumulation volumes. While we have demonstrated that the mean switching rate can be reduced to as low as 2 Hz, the switching must occur within milliseconds to ensure accuracy, as any time lag cannot be corrected in post-processing. The flow perturbations caused by the switching mechanism must also be minimized. Additionally, the system must be designed to minimize dead volumes and time lags. The accumulation volumes need to be optimized to provide sufficient sample quantities for the analyzer while accommodating the dynamic range of the accumulated samples. Many of these challenges are shared with the relaxed eddy accumulation method and are well documented in the literature [Ammann, 1998]. Meeting these requirements is fundamental to the successful deployment and operation of the QEA method.

By the end of the averaging interval, the flux can be calculated using Eq. 20 and corrected for nonzero \bar{w}_q if needed using Eq. 21. Since the measured quantities here are means rather than fluctuations, eddy accumulation methods are more robust to frequency losses due to the analyzer response and typically will not require spectral corrections [Emad, 2023].

5 Conclusions

In this paper, we introduced the quantized eddy accumulation (QEA) method with error diffusion, a new direct micrometeorological method with minimal implementation requirements. We framed the problem of flux measurement with conditional sampling at a constant flow rate as measuring the flux using a quantized wind signal. The conventional relaxed eddy accumulation (REA) method was identified as a special case of this framework, with biases in REA linked to the unaccounted flux portion transported by the covariance between the quantization error and scalar concentration.

This new formulation enabled us to develop an error diffusion algorithm that feeds quantization errors back into the signal, thereby driving the unaccounted flux term due to quantization errors to zero and eliminating the need for the empirical coefficient β . QEA with error diffusion aligns with eddy covariance and true eddy accumulation as a direct method while offering

the distinct advantage of enhancing the signal-to-noise ratio without compromising accuracy.

Our analysis and numerical simulations using high-frequency EC data from two contrasting ecosystems demonstrated that QEA has achieved unbiased flux estimates with errors below 0.1% over a wide range of quantization parameters and atmospheric conditions. Key technical challenges to the successful implementation of QEA include the need for fast-switching valves to direct flow between accumulation volumes, minimizing flow perturbations, and reducing time lags within the system.

The new method provides simple and reliable means for accurate flux measurements of challenging atmospheric constituents and has the potential to advance our understanding of atmospheric chemistry and earth science.

Data and code availability

The datasets generated and analyzed in this study, along with the full code implementation, are available at Emad [2024a] and the github repository <https://github.com/anase/quantized-eddy-accumulation>

Raw data for Braunschweig station that were used as input for the simulation are available at Emad [2024b].

Acknowledgements

I am grateful to the editor and reviewers for their comments and suggestions, which significantly improved this manuscript.

I acknowledge with gratitude the support of the Bioclimatology group led by Alexander Knohl at the University of Göttingen. I thank Lukas Siebicke for his guidance and valuable discussions on conditional sampling methods, and Anne Klosterhalfen for her assistance with the Hainich data.

I acknowledge the support by the German Federal Ministry of Education and Research (BMBF) as part of the European Integrated Carbon Observation System (ICOS). This work was partially funded by the Leibniz Association (Leibniz Collaborative Excellence Project ISO-SCALE), the Ministry of Lower Saxony for Science and Culture (MWK), and the Deutsche Forschungsgemeinschaft (INST 186/1118-1 FUGG).

References

- Dennis D. Baldocchi. How eddy covariance flux measurements have contributed to our understanding of Global Change Biology. *Global Change Biology*, 26(1):242–260, 2020. ISSN 1365-2486. doi:10.1111/gcb.14807.
- A. Arneth, S. P. Harrison, S. Zaehle, K. Tsigaridis, S. Menon, P. J. Bartlein, J. Feichter, A. Korhola, M. Kulmala, D. O’Donnell, G. Schurgers, S. Sorvari, and T. Vesala. Terrestrial biogeochemical feedbacks in the climate system. *Nature Geoscience*, 3(8):525–532, August 2010. ISSN 1752-0908. doi:10.1038/ngeo905.
- Mary Scholes, Patricia Matrai, Meinrat Andreae, Keith Smith, Martin Manning, Paulo Artaxo, Leonard Barrie, Timothy Bates, James Butler, Paolo Ciccioli, Stanislaw Cieslik, Robert Delmas, Frank

- Dentener, Robert Duce, David Erickson Iii, Ian Galbally, Alex Guenther, Ruprecht Jaenicke, Bernd Jähne, Anthony Kettle, Ronald Kiene, Jean-Pierre Lacaux, Peter Liss, G. Malin, Pamela Matson, Arvin Mosier, Heinz-Ulrich Neue, Hans Paerl, Ulrich Platt, Patricia Quinn, Wolfgang Seiler, and Ray Weiss. Biosphere-atmosphere interactions. In *Atmospheric Chemistry in a Changing World. An Integration and Synthesis of a Decade of Tropospheric Chemistry Research, Series Global Change, the IGBP Series*, pages 19–71. 2003. doi:10.1007/978-3-642-18984-5_2.
- D. Fowler, K. Pilegaard, M. A. Sutton, P. Ambus, M. Raivonen, J. Duyzer, D. Simpson, H. Fagerli, S. Fuzzi, J. K. Schjoerring, C. Granier, A. Neftel, I. S. A. Isaksen, P. Laj, M. Maione, P. S. Monks, J. Burkhardt, U. Daemmgen, J. Neiryneck, E. Personne, R. Wichink-Kruit, K. Butterbach-Bahl, C. Flechard, J. P. Tuovinen, M. Coyle, G. Gerosa, B. Loubet, N. Altimir, L. Gruenhage, C. Ammann, S. Cieslik, E. Paoletti, T. N. Mikkelsen, H. Ro-Poulsen, P. Cellier, J. N. Cape, L. Horváth, F. Loreto, Ü. Niinemets, P. I. Palmer, J. Rinne, P. Misztal, E. Nemitz, D. Nilsson, S. Pryor, M. W. Gallagher, T. Vesala, U. Skiba, N. Brüggemann, S. Zechmeister-Boltenstern, J. Williams, C. O’Dowd, M. C. Facchini, G. de Leeuw, A. Flossman, N. Chaumerliac, and J. W. Erisman. Atmospheric composition change: Ecosystems–Atmosphere interactions. *Atmospheric Environment*, 43(33):5193–5267, October 2009. ISSN 1352-2310. doi:10.1016/j.atmosenv.2009.07.068.
- W. F. Dabberdt, D. H. Lenschow, T. W. Horst, P. R. Zimmerman, S. P. Oncley, and A. C. Delany. Atmosphere-Surface Exchange Measurements. *Science*, 260(5113):1472–1481, June 1993. ISSN 0036-8075, 1095-9203. doi:10.1126/science.260.5113.1472.
- Bruce B. Hicks and Dennis D. Baldocchi. Measurement of Fluxes Over Land: Capabilities, Origins, and Remaining Challenges. *Boundary-Layer Meteorology*, 177(2):365–394, June 2020. ISSN 1573-1472. doi:10.1007/s10546-020-00531-y.
- Janne Rinne, Christof Ammann, Elizabeth Pattey, Kyaw Tha Paw U, and Raymond L. Desjardins. Alternative Turbulent Trace Gas Flux Measurement Methods. In Thomas Foken, editor, *Springer Handbook of Atmospheric Measurements*, Springer Handbooks, pages 1505–1530. Springer International Publishing, Cham, 2021. ISBN 978-3-030-52171-4. doi:10.1007/978-3-030-52171-4_56.
- R. L. Desjardins. Description and evaluation of a sensible heat flux detector. *Boundary-Layer Meteorology*, 11(2):147–154, March 1977. ISSN 1573-1472. doi:10.1007/BF02166801.
- B. B. Hicks and R. T. McMillen. A Simulation of the Eddy Accumulation Method for Measuring Pollutant Fluxes. *Journal of Climate and Applied Meteorology*, 23(4):637–643, April 1984. ISSN 0733-3021. doi:10.1175/1520-0450(1984)023<0637:ASOTEA>2.0.CO;2.
- Lukas Siebicke and Anas Emad. True eddy accumulation trace gas flux measurements: Proof of concept. *Atmospheric Measurement Techniques*, 12(8):4393–4420, August 2019. ISSN 1867-1381. doi:10.5194/amt-12-4393-2019.
- Joost A. Businger and Steven P. Oncley. Flux Measurement with Conditional Sampling. *Journal of Atmospheric and Oceanic Technology*, 7(2):349–352, April 1990. ISSN 0739-0572. doi:10.1175/1520-0426(1990)007<0349:FMWCS>2.0.CO;2.
- John M Baker. Conditional sampling revisited. *Agricultural and Forest Meteorology*, 104(1):59–65, July 2000. ISSN 0168-1923. doi:10.1016/S0168-1923(00)00147-7.
- Matsumoto Yukio and Utiyama Masahiro. A Statistical Derivation of the Fundamental Equations for the Relaxed Eddy Accumulation Method and the Properties of the b Coefficient. *Earozoru Kenkyu*, 19(4):266–272, 2004. doi:10.11203/jar.19.266.
- A.K. Fotiadi, F. Lohou, A. Druilhet, D. Serça, Y. Brunet, and R. Delmas. Methodological Development of the Conditional Sampling Method. Part I: Sensitivity to Statistical and Technical Characteristics. *Boundary-Layer Meteorology*, 114(3):615–640, March 2005. ISSN 1573-1472. doi:10.1007/s10546-004-1080-9.
- Johannes Ruppert, Christoph Thomas, and Thomas Foken. Scalar Similarity for Relaxed Eddy Accumulation Methods. *Boundary-Layer Meteorology*, 120(1):39–63, July 2006. ISSN 1573-1472. doi:10.1007/s10546-005-9043-3.
- G. Katul, O. Peltola, T. Grönholm, S. Launiainen, I. Mammarella, and T. Vesala. Ejective and Sweeping Motions Above a Peatland and Their Role in Relaxed-Eddy-Accumulation Measurements and Turbulent Transport Modelling. *Boundary-Layer Meteorology*, 2018. doi:10.1007/s10546-018-0372-4.
- Teresa Vogl, Amy Hrdina, and Christoph K. Thomas. Choosing an optimal β factor for relaxed eddy accumulation applications across vegetated and non-vegetated surfaces. *Biogeosciences*, 18(18):5097–5115, September 2021. ISSN 1726-4170. doi:10.5194/bg-18-5097-2021.
- John C. Wyngaard and Chin-Hoh Moeng. Parameterizing turbulent diffusion through the joint probability density. *Boundary-Layer Meteorology*, 60(1):1–13, July 1992. ISSN 1573-1472. doi:10.1007/BF00122059.
- W. Gao. The vertical change of coefficient b , used in the relaxed eddy accumulation method for flux measurement above and within a forest canopy. *Atmospheric Environment*, 29(17):2339–2347, September 1995. ISSN 1352-2310. doi:10.1016/1352-2310(95)00147-Q.
- Gabriel G. Katul, Peter L. Finkelstein, John F. Clarke, and Thomas G. Ellestad. An Investigation of the Conditional Sampling Method Used to Estimate Fluxes of Active, Reactive, and Passive Scalars. *Journal of Applied Meteorology and Climatology*, 35(10):1835–1845, October 1996. ISSN 1520-0450, 0894-8763. doi:10.1175/1520-0450(1996)035<1835:AIOTCS>2.0.CO;2.
- Jeng-Lin Tsai, Ben-Jei Tsuang, Pei-Hsuan Kuo, Chia-Ying Tu, Chi-Ling Chen, Ming-Tung Hsueh, Cheng-Shang Lee, Ming-Hwi Yao, and Mei-Li Hsueh. Evaluation of the relaxed eddy accumulation coefficient at various wetland ecosystems. *Atmospheric Environment*, 60:336–347, December 2012. ISSN 1352-2310. doi:10.1016/j.atmosenv.2012.06.081.
- Achim Grelle and Hannes Keck. Affordable relaxed eddy accumulation system to measure fluxes of H₂O, CO₂, CH₄ and N₂O from ecosystems. *Agricultural and Forest Meteorology*, 307:108514, September 2021. ISSN 0168-1923. doi:10.1016/j.agrformet.2021.108514.
- Ayaka Sakabe, Masahito Ueyama, Yoshiko Kosugi, Ken Hamotani, Takashi Hirano, and Ryuichi Hirata. Is the empirical coefficient b for the relaxed eddy accumulation method constant? *Journal of Atmospheric Chemistry*, 71(1):79–94, March 2014. ISSN 1573-0662. doi:10.1007/s10874-014-9282-0.
- C. Ammann and F. Meixner. Stability dependence of the relaxed eddy accumulation coefficient for various scalar quantities. *Journal of Geophysical Research: Atmospheres*, 107(D8):ACL7–1–ACL7–9, 2002. ISSN 2156-2202. doi:10.1029/2001JD000649.
- Steven P. Oncley, Anthony C. Delany, Thomas W. Horst, and Pieter P. Tans. Verification of flux measurement using relaxed eddy accumulation. *Atmospheric Environment. Part A. General Topics*, 27(15):2417–2426, October 1993. ISSN 0960-1686. doi:10.1016/0960-1686(93)90409-R.
- I. J. Beverland, J. B. Moncrieff, D. H. ÓNeill, K. J. Hargreaves, and R. Milne. Measurement of methane and carbon dioxide fluxes

- from peatland ecosystems by the conditional-sampling technique. *Quarterly Journal of the Royal Meteorological Society*, 122(532): 819–838, 1996. ISSN 1477-870X. doi:10.1002/qj.49712253203.
- S. Haapanala, J. Rinne, K.-H. Pystynen, H. Hellén, H. Hakola, and T. Riutta. Measurements of hydrocarbon emissions from a boreal fen using the REA technique. *Biogeosciences*, 3(1):103–112, March 2006. ISSN 1726-4170. doi:10.5194/bg-3-103-2006.
- David R. Bowling, Dennis D. Baldocchi, and Russell K. Monson. Dynamics of isotopic exchange of carbon dioxide in a Tennessee deciduous forest. *Global Biogeochemical Cycles*, 13(4):903–922, 1999. ISSN 1944-9224. doi:10.1029/1999GB900072.
- T. Zhu, D. Wang, R. L. Desjardins, and J. I. Macpherson. Aircraft-based volatile organic compounds flux measurements with relaxed eddy accumulation. *Atmospheric Environment*, 33(12):1969–1979, June 1999. ISSN 1352-2310. doi:10.1016/S1352-2310(98)00098-3.
- E. Pattey, R. L. Desjardins, H. Westberg, B. Lamb, and T. Zhu. Measurement of Isoprene Emissions over a Black Spruce Stand Using a Tower-Based Relaxed Eddy-Accumulation System. *Journal of Applied Meteorology*, 38(7):870–877, July 1999. ISSN 0894-8763. doi:10.1175/1520-0450(1999)038<0870:MOIEOA>2.0.CO;2.
- P. Ciccioli, E. Brancaleoni, M. Frattoni, S. Marta, A. Brachetti, M. Vitullo, G. Tirone, and R. Valentini. Relaxed eddy accumulation, a new technique for measuring emission and deposition fluxes of volatile organic compounds by capillary gas chromatography and mass spectrometry. *Journal of Chromatography. A*, 985(1-2): 283–296, January 2003. ISSN 0021-9673. doi:10.1016/s0021-9673(02)01731-4.
- Kazuhide Matsuda, Ichiro Watanabe, Kou Mizukami, Satomi Ban, and Akira Takahashi. Dry deposition of PM_{2.5} sulfate above a hilly forest using relaxed eddy accumulation. *Atmospheric Environment*, 107:255–261, April 2015. ISSN 1352-2310. doi:10.1016/j.atmosenv.2015.02.050.
- A. Hensen, E. Nemitz, M. J. Flynn, A. Blatter, S. K. Jones, L. L. Sørensen, B. Hensen, S. C. Pryor, B. Jensen, R. P. Otjes, J. Cobussen, B. Loubet, J. W. Erisman, M. W. Gallagher, A. Nefitel, and M. A. Sutton. Inter-comparison of ammonia fluxes obtained using the Relaxed Eddy Accumulation technique. *Biogeosciences*, 6(11):2575–2588, November 2009. ISSN 1726-4170. doi:10.5194/bg-6-2575-2009.
- Henrik Skov, Steven B. Brooks, Michael E. Goodsite, Steve E. Lindberg, Tilden P. Meyers, Matthew S. Landis, Michael R. B. Larsen, Bjarne Jensen, Glen McConville, and Jesper Christensen. Fluxes of reactive gaseous mercury measured with a newly developed method using relaxed eddy accumulation. *Atmospheric Environment*, 40(28):5452–5463, September 2006. ISSN 1352-2310. doi:10.1016/j.atmosenv.2006.04.061.
- T. P. Meyers, W. T. Luke, and J. J. Meisinger. Fluxes of ammonia and sulfate over maize using relaxed eddy accumulation. *Agricultural and Forest Meteorology*, 136(3):203–213, February 2006. ISSN 0168-1923. doi:10.1016/j.agrformet.2004.10.005.
- S. Osterwalder, J. Fritsche, C. Alewell, M. Schmutz, M. B. Nilsson, G. Jocher, J. Sommar, J. Rinne, and K. Bishop. A dual-inlet, single detector relaxed eddy accumulation system for long-term measurement of mercury flux. *Atmospheric Measurement Techniques*, 9(2):509–524, February 2016. ISSN 1867-1381. doi:10.5194/amt-9-509-2016.
- Andreas Held, Edward Patton, Luciana Rizzo, Jim Smith, Andrew Turnipseed, and Alex Guenther. Relaxed Eddy Accumulation Simulations of Aerosol Number Fluxes and Potential Proxy Scalars. *Boundary-Layer Meteorology*, 129(3):451–468, December 2008. ISSN 1573-1472. doi:10.1007/s10546-008-9327-5.
- Tiia Grönholm, Pasi P. Aalto, Vei Jo Hiltunen, Üllar Rannik, Janne Rinne, Lauri Laakso, Saara Hyvönen, Timo Vesala, and Markku Kulmala. Measurements of aerosol particle dry deposition velocity using the relaxed eddy accumulation technique. *Tellus B: Chemical and Physical Meteorology*, 59(3):381–386, January 2007. ISSN null. doi:10.1111/j.1600-0889.2007.00268.x.
- K. E. Hornsby, M. J. Flynn, J. R. Dorsey, M. W. Gallagher, R. Chance, C. E. Jones, and L. J. Carpenter. A Relaxed Eddy Accumulation (REA)-GC/MS system for the determination of halocarbon fluxes. *Atmospheric Measurement Techniques*, 2(2):437–448, August 2009. ISSN 1867-1381. doi:10.5194/amt-2-437-2009.
- X Ren, J E Sanders, A Rajendran, R J Weber, A H Goldstein, S E Pusede, E C Browne, K.-E Min, and R C Cohen. A relaxed eddy accumulation system for measuring vertical fluxes of nitrous acid. *Atmos. Meas. Tech*, 4:2093–2103, 2011. doi:10.5194/amt-4-2093-2011.
- A. Moravek, T. Foken, and I. Trebs. Application of a GC-ECD for measurements of biosphere–atmosphere exchange fluxes of peroxyacetyl nitrate using the relaxed eddy accumulation and gradient method. *Atmospheric Measurement Techniques*, 7(7):2097–2119, July 2014. ISSN 1867-1381. doi:10.5194/amt-7-2097-2014.
- N. Meskhidze, T. M. Royalty, B. N. Phillips, K. W. Dawson, M. D. Petters, R. Reed, J. P. Weinstein, D. A. Hook, and R. W. Wiener. Continuous flow hygroscopicity-resolved relaxed eddy accumulation (Hy-Res REA) method of measuring size-resolved sodium chloride particle fluxes. *Aerosol Science and Technology*, 52(4):433–450, April 2018. ISSN 0278-6826. doi:10.1080/02786826.2017.1423174.
- Guilherme Calabro-Souza, Andreas Lorke, Christian Noss, Philippe Dubois, Mohamed Saad, Celia Ramos-Sanchez, Brigitte Vinçon-Leite, Régis Moilleron, Magali Jodeau, and Bruno J. Lemaire. A New Technique for Resolving Benthic Solute Fluxes: Evaluation of Conditional Sampling Using Aquatic Relaxed Eddy Accumulation. *Earth and Space Science*, 10(9):e2023EA003041, 2023. ISSN 2333-5084. doi:10.1029/2023EA003041.
- M. Riederer, J. Hübner, J. Ruppert, W. A. Brand, and T. Foken. Prerequisites for application of hyperbolic relaxed eddy accumulation on managed grasslands and alternative net ecosystem exchange flux partitioning. *Atmospheric Measurement Techniques*, 7(12): 4237–4250, December 2014. ISSN 1867-1381. doi:10.5194/amt-7-4237-2014.
- J. J. Finnigan, R. Clement, Y. Malhi, R. Leuning, and H.A. Cleugh. A Re-Evaluation of Long-Term Flux Measurement Techniques Part I: Averaging and Coordinate Rotation. *Boundary-Layer Meteorology*, 107(1):1–48, April 2003. ISSN 1573-1472. doi:10.1023/A:1021554900225.
- Thomas Foken, Marc Aubinet, and Ray Leuning. The Eddy Covariance Method. In Marc Aubinet, Timo Vesala, and Dario Papale, editors, *Eddy Covariance: A Practical Guide to Measurement and Data Analysis*, Springer Atmospheric Sciences, pages 1–19. Springer Netherlands, Dordrecht, 2012. ISBN 978-94-007-2351-1. doi:10.1007/978-94-007-2351-1_1.
- Anas Emad and Lukas Siebicke. True eddy accumulation – Part 1: Solutions to the problem of non-vanishing mean vertical wind velocity. *Atmospheric Measurement Techniques*, 16(1):29–40, January 2023a. ISSN 1867-1381. doi:10.5194/amt-16-29-2023.
- Andrew S. Kowalski. The boundary condition for vertical velocity and its interdependence with surface gas exchange. *Atmospheric Chemistry and Physics*, 17(13):8177–8187, July 2017. ISSN 1680-7316. doi:10.5194/acp-17-8177-2017.
- Andrew S. Kowalski, Penélope Serrano-Ortiz, Gabriela Miranda-García, and Gerardo Fratini. Disentangling Turbulent Gas Diffusion

- from Non-diffusive Transport in the Boundary Layer. *Boundary-Layer Meteorology*, 179(3):347–367, June 2021. ISSN 1573-1472. doi:[10.1007/s10546-021-00605-5](https://doi.org/10.1007/s10546-021-00605-5).
- Keith T. Knox. Evolution of error diffusion. *Journal of Electronic Imaging*, 8(4):422–429, October 1999. ISSN 1017-9909, 1560-229X. doi:[10.1117/1.482710](https://doi.org/10.1117/1.482710).
- T.D. Kite, B.L. Evans, A.C. Bovik, and T.L. Sculley. Digital halftoning as 2-D delta-sigma modulation. In *Proceedings of International Conference on Image Processing*, volume 1, pages 799–802 vol.1, October 1997. doi:[10.1109/ICIP.1997.648084](https://doi.org/10.1109/ICIP.1997.648084).
- R. Escbbach, Z. Fan, K.T. Knox, and G. Marcu. Threshold modulation and stability in error diffusion. *IEEE Signal Processing Magazine*, 20(4):39–50, July 2003. ISSN 1558-0792. doi:[10.1109/MSP.2003.1215230](https://doi.org/10.1109/MSP.2003.1215230).
- Julius Smith. *Introduction to Digital Filters with Audio Applications*. W3K Publishing, 2007. ISBN 978-0-9745607-1-7.
- T. D. Kite, B. L. Evans, and A. C. Bovik. Modeling and quality assessment of halftoning by error diffusion. *IEEE transactions on image processing: a publication of the IEEE Signal Processing Society*, 9(5):909–922, 2000. ISSN 1057-7149. doi:[10.1109/83.841536](https://doi.org/10.1109/83.841536).
- Anas Emad and Lukas Siebicke. True eddy accumulation – Part 2: Theory and experiment of the short-time eddy accumulation method. *Atmospheric Measurement Techniques*, 16(1):41–55, January 2023b. ISSN 1867-1381. doi:[10.5194/amt-16-41-2023](https://doi.org/10.5194/amt-16-41-2023).
- Alexander Knohl, Ernst-Detlef Schulze, Olaf Kolle, and Nina Buchmann. Large carbon uptake by an unmanaged 250-year-old deciduous forest in Central Germany. *Agricultural and Forest Meteorology*, 118(3):151–167, 2003. ISSN 01681923. doi:[10.1016/S0168-1923\(03\)00115-1](https://doi.org/10.1016/S0168-1923(03)00115-1).
- Thomas Foken, Mathias Göockede, Matthias Mauder, Larry Mahrt, Brian Amiro, and William Munger. Post-Field Data Quality Control. In Xuhui Lee, William Massman, and Beverly Law, editors, *Handbook of Micrometeorology: A Guide for Surface Flux Measurement and Analysis*, Atmospheric and Oceanographic Sciences Library, pages 181–208. Springer Netherlands, Dordrecht, 2005. ISBN 978-1-4020-2265-4. doi:[10.1007/1-4020-2265-4_9](https://doi.org/10.1007/1-4020-2265-4_9).
- Anas Emad. Data and support code for the paper: 100-fold improvement in relaxed eddy accumulation flux estimates through error diffusion, May 2024a.
- Timo Gnamb. A brief note on the standard error of the Pearson correlation, April 2022.
- Douglas G. Bonett and Thomas A. Wright. Sample size requirements for estimating pearson, kendall and spearman correlations. *Psychometrika*, 65(1):23–28, March 2000. ISSN 1860-0980. doi:[10.1007/BF02294183](https://doi.org/10.1007/BF02294183).
- E. Pattey, R. L. Desjardins, and P. Rochette. Accuracy of the relaxed eddy-accumulation technique, evaluated using CO₂ flux measurements. *Boundary-Layer Meteorology*, 66(4):341–355, December 1993. ISSN 1573-1472. doi:[10.1007/BF00712728](https://doi.org/10.1007/BF00712728).
- Christof Ammann. *On the Applicability of Relaxed Eddy Accumulation and Common Methods for Measuring Trace Gas Surface Fluxes*. Doctoral Thesis, ETH Zurich, 1998.
- Anas Emad. Optimal Frequency-Response Corrections for Eddy Covariance Flux Measurements Using the Wiener Deconvolution Method. *Boundary-Layer Meteorology*, 188(1):29–53, July 2023. ISSN 1573-1472. doi:[10.1007/s10546-023-00799-w](https://doi.org/10.1007/s10546-023-00799-w).
- Anas Emad. High-frequency wind (u, w, v, Ts) and gas concentration measurements of CO₂ and H₂O over an agricultural field in Braunschweig, Germany, May 2024b.